Journal of Materials Science and Engineering A 11 (4-6) (2021) 48-55
doi: 10.17265/2161-6213/2021.4-6.003

Effect of Molecular Structure on Diffusion of Alcohols through Type-A Zeolite Pores (0.5 nm)

Bryan Fernández-Solano and Julio F. Mata-Segreda

Biomass Laboratory, School of Chemistry, University of Costa Rica 11501-2060, Costa Rica

Abstract: Drying kinetics for alcohol-soaked type-A zeolite (pore size 0.5 nm) was determined at 50 °C for 12 small-molecule alcohols (from C_1 to C_{10}). The second-phase of drying of wet porous materials reports on the mass-transfer characteristics within the solid matrices. This stage follows pseudo first-order kinetics (k_1), and the second-order rate constant $k_2 = k_1$/(fluxional area) was found to correlate with the surface tension of the liquids imbibing the solid matrix ($p < 0.002$). k_2 values decrease along the homologous linear alcohols, and branched-chain alcohols diffuse faster than their linear analogues due to their lower surface tensions. No independent contribution was found from the molecular size of the alcohols in the experiment reported here. Characteristic velocity and enthalpy of vaporisation of the liquids were not found to be significant independent variables, either. The find agrees with the notion that liquid movement in pores is governed during the drying processes by the liquid chemical potential gradient between the pore space and gas phase above the porous particle surfaces, this gradient being a function of the molecular cohesion of the moving liquid front (surface tension, γ). The results can be expressed by the linear Gibbs-energy relation $\log (k_2/s^{-1}\cdot m^{-2}) = (2.5 \pm 0.5) - (1.6 \pm 0.2) \times 10^2$ (γ/J·m^{-2}).

Key words: Drying kinetics, liquid diffusion through pores, surface tension, heterogeneous catalysis.

1. Introduction

Diffusion of fluids through porous materials is a significant molecular event in many operations and processes such as biomass combustion and gasification [1, 2], drying of porous materials [3], heterogeneous catalysis [4-6], pollutant diffusion in soils [7], and the separation and storage of fluids [8-10]. The use of heterogeneous catalysts is important for the improvement of process energy requirements in industry as well as in the laboratory because it makes easier the disposition of residues, and minimises the number of steps for the isolation and purification of the desired end products. A kinetic aspect such as contact time of feedstocks with catalyst is also an easier operation to manage.

The activity, selectivity and specificity of heterogeneous catalysts depend on the volumetric porosity of support materials and pore characteristics such as dimensions and tortuosity. Heterogeneous catalysts may be envisioned as pseudo-homogeneous phases, where reacting species undergo a hindering effect on their movement due to partial obstruction of the cross-sectional area by the solid materials, and longer diffusion routes because molecules must wind their way around the obstructions (tortuosity effect).

The magnitude of the diffusional retardation can be assessed by the use of an effective mass-transfer (or diffusivity) coefficient. This parameter is the quotient of the diffusivity of a moving species in the pores, relative to the same quantity in the bulk liquid state, at a particular temperature. This physical property is stated as dependent on the volumetric porosity of the solid matrix (ε), the constrictivity or bottle-neck effect (σ) and the tortuosity of the pores (τ) [5, 11]:

$$\frac{D_{pore}}{D_{liquid}} = \frac{\epsilon \times \sigma}{\tau} \quad (1)$$

ε is the fraction of empty volume inside the solid porous matrix. Because the pores in the matrix are not cylindrical and straight, but interconnected ducts and

Corresponding author: Julio F. Mata-Segreda, Ph.D., professor, research fields: catalysis and renewable energy.

have varying cross-sectional areas perpendicular to the fluid flow, the narrower sites exert a "bottle-neck" effect on diffusion, a feature specified by σ. As in a winding rural road, τ is formally defined as the actual distance molecules travel in pores in order to diffuse from a point A to B, relative to the shortest distance between those two points. Typical values of these parameters are ε~0.4, σ~0.8 and τ~3 [5]. Therefore, the overall diffusional effect is of one order of magnitude [5, 6]: D_{pore}/D_{liquid}~10^{-1}.

It was pointed out above that the specificity and selectivity of heterogeneous catalysts are dependent on the mass-transfer resistance of either reagents and products. Consequently, from a microscopic point of view, it is understood that the well-known occurrence of *shape-selective catalysis* depends on the dimensions and shapes of pores in the catalyst-support matrices and the geometry of reactant and product molecules. Therefore, it is of interest to explore the effect of molecular structural features of moving particles on their diffusion in pores.

This paper gives the kinetic parameters for the drying operation decreasing-rate stage of type-A zeolite (0.5 nm) imbibed with different short-chain alcohols (C_1-C_{10}) at 50 °C and 87 kPa atmospheric pressure. This experiment was designed as an empirical model for mass-transfer of liquid materials in pores, and its relevancy to heterogeneous catalysis is independent of the situation whether chemical reactions occur or not.

2. Experiment

2.1 Materials

Type-A zeolite with 0.5 nm pores was purchased from Sigma-Aldrich as 1.6 mm pellets. The different alcohols were common chemicals obtained from the shelf in the stockroom of the School of Chemistry, University of Costa Rica.

2.2 Drying Curves

Ohaus MB 35 Halogen Moisture Analysers (Ohaus Corporation, 19A Chapin Road, Pine Brook, N.J., USA) were used to measure the time-mass data for the drying curves. The runs were carried out at 50 °C and 87 kPa atmospheric pressure. The relative humidity of the laboratory environment was maintained in the range of 60%-70%.

The zeolite samples were soaked with each of the alcohols studied for 14 h-17 h prior to the gravimetric measurements. The wet solids were gently pressed between paper towel plies, in order to obtain free-flowing solids. 10-gramme samples were placed on 74 cm^2 aluminium-foil plates, and the time-mass data were recorded until constant weight was reached at 50 °C. Each run was carried out in triplicate, and uncertainty limits were given as standard errors from the average.

2.3 Data Treatment

The rates of evaporation of the pure liquids were determined gravimetrically by using the drying balances described above.

For the drying experiments, the extent of drying was calculated as $x = [m(0) - m(t)]/[m(0) - m(\infty)]$. The first constant-rate stage ($-dm/dt$ = constant) was determined from linear least-squares fitting in the period with Pearson's $|r_p| \geq 0.9990$.

The apparent pseudo first-order rate constant in the second drying stage was calculated as the slope of dx/dt vs. $(1 - x)$ that follows a linear relationship (*vide infra*). The values of dx/dt were calculated from fitting cubic polynomials $x = f(t)$. Fluxional areas for every alcohol/zeolite run were obtained from their molecular masses M and rates of evaporation of the pure alcohols r_{evap} at 50 °C and 87 kPa:

$$\text{Fluxional area} = \frac{\left(\frac{-dm}{dt}\right)_{initial} gs^{-1}}{Mgmol^{-1} \times r_{evap} mols^{-1}m^{-2}} \quad (2)$$

3. Results and Discussion

Drying is a process dependent on heat and mass transfer factors. Therefore, a study on a drying operation such as the one reported in this account,

must be carried out by fixing the heat-transfer variable. The use of the indicated drying balance achieves this objective, because the instrument is constructed with a halogen heating element that provides constant and uniform infrared heating of the sample in the sample compartment.

The kinetics of drying of porous materials against a stagnant gaseous surrounding allows gaining molecular inferences about the movement of liquids through pores. Experiments with different liquids make possible establishing empirical guidelines about the relationship between the structural molecular characteristics of liquids in porous solids and their diffusional dynamics, a kind of useful information for heterogeneous catalysis, storage of liquids in porous solids and other operations and processes.

Table 1 gives the absolute rates of evaporation of the pure liquids studied in this work, at 50 °C and 87 kPa. Data for liquid H_2O are included for comparison.

The kinetic law that describes the evaporation of a pure liquid against a stagnant gaseous surrounding is 0th-order, as indicated by the Hertz-Knudsen equation [12]:

$$\frac{-dn_{liquid}/dt}{Area} = \kappa \frac{p_v(T)}{\sqrt{2\pi\, M\, RT}} \qquad (3)$$

where κ is a transmission factor that accounts for the fraction of the liquid molecules that remain in the gaseous phase after evaporation, $p_v(T)$ is the liquid vapour pressure at temperature T, M stands for the molecular mass of the liquid material and RT has the usual meaning.

The rate of evaporation of the different alcohols (ROH) decreases as the number of carbon atoms increases, as expected from enhanced non-polar interactions in the liquid phase. For molecules with the same number of carbon atoms, the rate of evaporation increases for branched molecules, a feature also predictable based on the same molecular grounds since branched structures possess smaller molecular areas than their linear counterparts, and thus lower degree of attraction in the liquid phase.

Table 1 Absolute rates of evaporation of the pure liquids studied in this work, 50 °C.

Liquid	Rate of evaporation, 50 °C/mmol $s^{-1}\cdot m^{-2}$
MeOH	15.4 ± 0.5
EtOH	9.8 ± 0.3
n-PrOH	4.96 ± 0.02
i-PrOH	8.3 ± 0.2
n-BuOH	2.6 ± 0.2
i-BuOH	2.84 ± 0.05
s-BuOH	4.1 ± 0.2
t-BuOH	6.4 ± 0.2
n-AmOH	1.4 ± 0.1
i-AmOH	1.81 ± 0.01
Geraniol	0.0942 ± 0.0007
H_2O	11.4 ± 0.2

Fig. 1 shows the Krischer drying curve of ethanol-soaked type-A zeolite (0.5 nm pore) as an example at 50 °C and 87 kPa, against the nearly stagnant gaseous environment of the laboratory. All curves obtained in this study share qualitatively the same common features discussed here for EtOH/zeolite A.

For ethanol, the typical constant-rate stage extends up to the critical degree of drying x_c = 0.55. The mechanistic interpretation of this initial kinetic phase is of full liquid coverage of the solid particles that behave analogously to the free surface of liquids. This kinetic behaviour occurs whilst the rate of liquid evaporation from the surface is counterbalanced by the rate of arrival of inner fluid molecules at the particle surface [13].

After (1 - x_c) is reached, dx/dt decreases in proportion to the fraction of remaining fluid in the porous matrix, up to x = 0.9. This second kinetic phase is now described by a pseudo first-order rate equation:

$$\frac{dx}{dt} = k_1(1-x) \qquad (4)$$

This observation reveals that the kinetics is defined now by internal transport that depends on the characteristics of pores in the solid material, contrary to the constant-rate period where molecular mass and intrinsic volatility of the liquid (vapour pressure) are the significant factors.

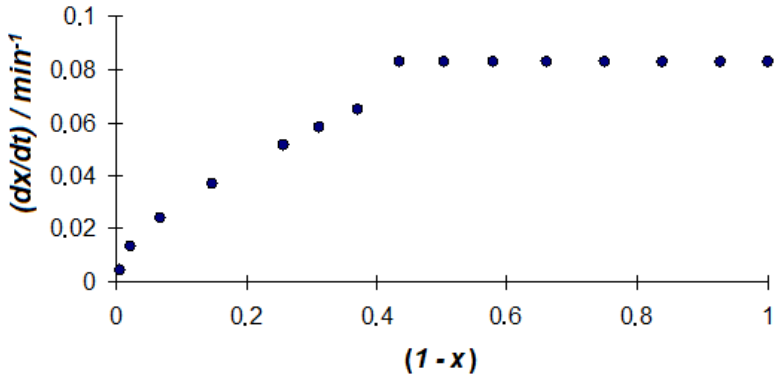

Fig. 1 Krischer drying curve for ethanol-imbibed type A zeolite (0.5 nm) at 50 °C and 87 kPa.

Table 2 Second-order rate constants for the drying of alcohols imbibed in zeolite type A (0.5 nm) at 50 °C and 87 kPa.

Liquid	10^2 surface tension/J·m^{-2}	10^6 van der Waals volume/m^3·mol^{-1}	10^2 k_2/s^{-1}·m^{-2}
MeOH	2.014	21.71	21 ± 4
EtOH	1.979	31.94	33 ± 7
n-PrOH	2.131	42.17	23 ± 3
i-PrOH	1.869	42.16	37 ± 4
n-BuOH	2.21	52.40	13 ± 2
i-BuOH	2.05	52.39	12 ± 4
s-BuOH	2.08	52.39	14 ± 9
t-BuOH	1.80	52.38	36 ± 4
n-AmOH	2.31	62.63	8 ± 1
i-AmOH	2.21	62.62	17 ± 2
n-HxOH	2.33	72.86	2.84 ± 0.04
Geraniol	2.67	185.07	2.0 ± 0.3
H_2O	6.791	10.83	13 ± 5

Mass-transfer dynamics in the pores can be assessed by the second-order rate constant $k_2 = k_1$/(fluxional area). It is possible to detect sometimes a third more complex kinetic phase at high degrees of drying, depending on the nature of the liquid and porous material (x greater than 0.9 for the case of EtOH).

Table 2 contains the corresponding k_2, surface tensions and van der Waals volumes of the liquids included in this study. The surface tensions at the working temperature were calculated from literature data (commonly at 20 °C) and the critical temperatures of the ROH, by using the Guggenheim-Katayama equation.

Movement of liquids in pores may occur by diffusion driven by concentration gradients produced by the exhaustion of liquid at the particle surface due to evaporation. Other mechanisms may be the action of capillary forces or a series of vaporisations and condensations in the pore space.

Thus, based on purely intuitive rationale, one could think of four physical properties on which the dynamics of liquid diffusion in pores might depend on: viscosity, enthalpy of vaporisation, molecular size, and surface tension. The following are three considerations that allow setting a simple mechanistic model to understand the results given in Table 2.

(1) Consideration 1

If capillary spreading was the most significant acting mechanism, as liquids advance through a pore, their ability to maintain contact with the walls results from the intermolecular forces established when the

two are in contact. The resulting degree of wetting (liquid advancement through pores) would be governed by the balance between cohesive and adhesive forces. The "pulling" effect wielded by the surface tension at the meniscus area is inversely related to the "drag" exerted by the liquid viscosity along the pore length. The parameter known as characteristic velocity = surface tension/viscosity controls the dynamics of wetting [14, 15]. An attempt to correlate log k_2 (proportional to the Gibbs-energy barrier) with the characteristic velocities for the substances studied in this work yielded no statistically significant result, with a Pearson's correlation coefficient r_P = 0.23. Thus, for the system at hand, the characteristic velocity is not a significant independent variable.

(2) Consideration 2

The same numerical exercise was done for the case of the enthalpy of vaporisation yielding r_P = 0.72 (p = 0.02). The situation is different from the correlation of log (rate of evaporation) and $\Delta_{vap}H$ of the pure free liquids with r_P = 0.98, p < 0.005. This last result is expected from Eq. (3) and the Clausius-Clapeyron equation. So, there must be other more significant factors for the diffusion of these liquids in pores, than the overall cohesive forces in the in-pore liquid ($\Delta_{vap}H$).

(3) Consideration 3

It is therefore pertinent to explore the specific effect of liquid cohesion at the traveling front (surface tension, γ) and molecular size (van der Waals volume, V_{vdW}). A simple analysis of variance check was carried out between the Gibbs-energy of activation for movement in the pores (proportional to log k_2) as a dependent variable and the surface tension of the liquids at 50 °C (γ) and their van der Waals volumes [16] as independent variables. By using Excel, one obtains:

$$\log k_2 = (2.2 \pm 0.7) - (1.2 \pm 0.4) \times 10^2 \gamma - (7 \pm 5) \times 10^3 V_{vdW} \quad (5)$$

The statistical certainty parameters for the three terms in Eq. (5) are p = 0.02, p = 0.02 and p = 0.2, respectively. This clearly indicates that molecular size exerts no independent contribution on k_2 compared to γ. Thus, the one-independent variable relation results:

$$\log k_2 = (2.6 \pm 0.7) - (1.6 \pm 0.3) \times 10^2 \gamma \quad (6)$$

The confidence parameters are now p = 0.006 and p = 0.001. The difference in molecular size between MeOH and *n*-HxOH is 236%, a condition probably not sufficient to detect any effect from their sizes in 0.5 nm pores. The same can be said for the γ values amongst isomers. The r_P of Eq. (6) though statistically meaningful is modest, $|r_P|$ = 0.84, p = 0.01. An additional experiment was done, in order to test the validity of Eq. (6). This equation predicts a value k_2 (50 °C) = 2.1 × 10^{-2} s^{-1}·m^{-2} for geraniol, a terpene (C_{10}) alcohol. The experiment yielded a value k_2 (50 °C) = (2.0 ± 0.3) × 10^{-2} s^{-1}·m^{-2} in good agreement with the expectation value. Incorporation of this last value gives the regression equation:

$$\log k_2 = (2.5 \pm 0.5) - (1.6 \pm 0.2) \times 10^2 \gamma \quad (7)$$

with a $|r_P|$ = 0.91. Since the uncertainties associated to the k_2 values are around 3%; the obtained r_P value can be accepted as index of a valid regression equation.

Fig. 2 shows the correlation stated by Eq. (7).

There is one point that needs further discussion. Why is the log k_2 - γ a better correlation than log k_2 - $\Delta_{vap}H$, (r_P = 0.91 vs. r_P = 0.72) since the magnitude of both γ and $\Delta_{vap}H$ is related to molecular structure as it is clear from simple inspection of databases?

A basic comment on the nature of γ is necessary to account for this third consideration. To extend the area of the vapour-wall-liquid interphases, it is required to transport molecules from the in-pore bulk into the meniscus surface. This process demands work to be done against the cohesive forces in the liquid. Thus, γ certainly depends upon intermolecular attractions and hence upon the enthalpy of vaporization [17]. In the bulk liquid phase, molecules interact with all neighbouring molecules around, but surface molecules interact only with their two-dimensional surface neighbours and those below the surface. For the advancement of the liquid front in the matrix pores, orientational effects on intermolecular interactions (γ)

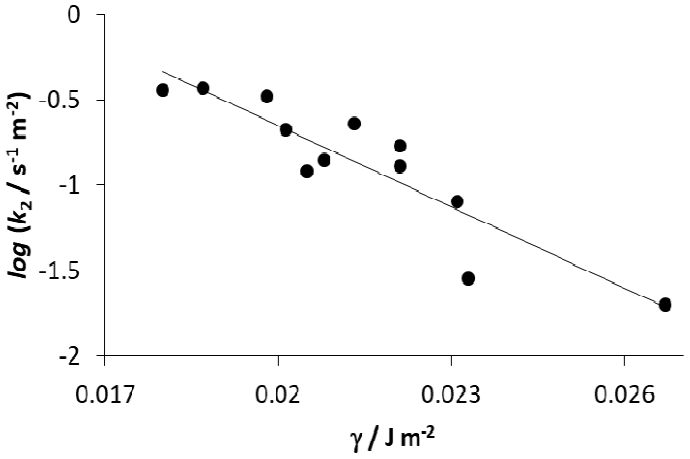

Fig. 2 Linear Gibbs-energy relationship between the alcohols surface tension and diffusional dynamics in the pores of type-A zeolite (0.5 nm) at 50 °C.

are more significant at the surface than in three-dimensional liquid bulk ($\Delta_{vap}H$). It is therefore conceivable that γ be a better descriptor than $\Delta_{vap}H$. From the molecular viewpoint, one can state that the activation Gibbs energy for flow in pores (proportional to log k_2) depends on the liquid cohesion at the meniscus region in a particular solid medium.

The more theoretically-approached study of Sharma and Debenedetti [18] on the evaporation rate of H_2O confined in nanometric hydrophobic spaces, leads to a similar conclusion. Those authors found that the Gibbs-energy barrier to evaporation of water correlates linearly with line tension as the predominant contribution. The Gibbs energy of a one-component system varies at fixed temperature according to the basic thermodynamic rationale [19]:

$$dG = V\,dp + \sum \gamma_i\,dS_i + \lambda\,dL \qquad (8)$$

where V is the system volume, γ_i and S_i are the interfacial tensions and areas, and λ is the line tension along the contact line length L. The last two Gibbs-energy derivatives (γ and λ) are related *via* the so-called tension length, $l = -\lambda/\gamma$ [19].

A mechanical picture of λ is the force operating along a three-phase line, that is, the intersection of three phases. In the case at hand, it involves the contact of the liquid with the pore wall and its immediate vapour within the pore space. The negative sign arises from the fact that λ can be either positive or negative. A positive λ value operates to constrict the length of the three-phase line, and a negative value tends to expand it. Both γ and λ result from attractive interactions at interphases [19]. Since λ is proportional to γ, the result of Sharma and Debenedetti [18] and our phenomenological observation agree.

The effect of molecular shape on diffusion in bulk liquid phase has been studied by Vasanthi et al. [20] and Chan et al. [21]. The proposed mechanisms were combinations of linear movements as well as coupled linear and rotational modes. Ghorai et al. [22] studied the diffusion of linear hydrocarbons through NaY zeolite with 0.75 nm pores *via* molecular dynamics and found that it is dependent on the sizes of the diffusing entities and pores. Those authors found that diffusivity is maximum when the length of the linear molecule matched the diameter of the bottle neck through which it is passing. No intuitive mechanistic details were discussed by the authors.

Thus it is suggestive that liquid advance in nanoconfinement during drying processes depends on the fluid chemical potential gradient between the pore space and gas phase above the porous particle surfaces, a notion that checks adequately with the linear Gibbs-energy relationship found in this work.

4. Conclusions

(a) Drying kinetics is an approach simple enough for the understanding of processes that involve the diffusivity of liquids in confined spaces during drying processes. The study of liquid diffusivity in pores *per se* is of significant importance for heterogeneous catalysis, independently of the occurrence of chemical reactions.

(b) The results described in this work are useful for the choice and design of heterogeneous catalysts, with special consideration to shape-selective catalysis, that is, catalysts that favour the formation of certain products because they can distinguish between the reactant, product or transition-state complex in terms of relative shape and size of the reacting species and the pore space where the reaction occurs [23].

(c) The second-order rate constant for the variable-rate stage of the drying operation (k_2) decreases along the homologous linear ROH series.

(d) Branched-chain ROH diffuses faster than their linear analogues.

(e) The surface tension of the liquids was found to be a significant independent variable that defines diffusivity of the liquids studied, in the 0.5 nm pores of type-A zeolite at 99% statistical certainty.

(f) The molecular size of the group of ROH studied plays no direct effect on diffusivity kinetics in the 0.5 nm pores of type-A zeolite at 50 °C, compared to the effect of γ.

(g) Characteristic velocity and enthalpies of vaporisation of the liquids were found of null or lesser significance relative to γ, as independent variables for log k_2.

Acknowledgements

The authors acknowledge the material support from the School of Chemistry Stockroom, UCR.

References

[1] Shivaku, R., and Maitra, S. 2019. "Evaluation of Pore Size and Surface Morphology during Devolatilization of Coconut Fibre and Sugar Cane Bagasse." *Combust. Sci. Technol.* doi: 10.1080/00102202.299019.1645655.

[2] Fatehi, H., and Bai, X.-S. 2015. "Effect of Pore Size on the Gasification of Biomass Char." *Energy Procedia* 75: 779-85.

[3] Puente-Urbina, A., Morales-Aymerich, J. P., Kim, Y. S., and Mata-Segreda, J. F. 2016. "Drying Kinetics as Assessment of Relative Energy Cost for Drying of Woody Biomasses." *Int. J. Renew. Energy & Biofuels*. doi: 10.5171/2016.701233.

[4] Helfferich, F. G. 2004. "Heterogeneous Catalysis." In *Comprehensive Chemical Kinetics*, vol. 40, chapter 9, 2nd ed., Elsevier, 273-308.

[5] Fogler, H. S. 2001. *Elementos de Ingeniería de las Reacciones Químicas*. Chapter 11, 3rd Spanish ed., Mexico: Pearson Education, 738-46.

[6] Conejo-Barboza, G., and Mata-Segreda, J. F. 2018. "Drying Kinetics as Tool for the Assessment of Dynamic Porosity of Catalyst-Support Materials." *Int. J. Renew. Energy & Biofuels.* doi: 10.5171/2018.901967.

[7] Zhou, C., Liu, C., Liang, J., and Wang, S. 2018. "Numerical Simulation of Pollutant Transport in Soils Surrounding Subway Infrastructure." *Environ. Sci. Pollution Res*. 25: 6859-69.

[8] Yabushita, M., Li, P., Kobayashi, H., Fukuoka, A., Farha, O. K., and Katz, A. 2016. "Complete Furanics-Sugar Separations with Metal-Organic Framework NU-1000." *Chem. Commun.* 52: 11791-4.

[9] Kim, J., Maiti, A., Lin, L.-C., Stolaroff, J. K., Smit, B., and Aines, R. D. 2013. "New Materials for Methane Capture from Dilute and Medium Sources." *Nature Commun.* 4: 1694. doi: 10.1038/ncomms2697.

[10] Song, Z., Nambo, A., Tate, K. L., Bas, A., Zhu, M., Jasinski, J. B., Zhou, S. J., Meyer, H. S., Carreon, M. A., Li, S., and Yu, M. 2016. "Nanovalved Adsorbents for CH_4 Storage." *Nano Letters* 16: 3309-13.

[11] Mezedur, M. M., Kaviany, M., and Moore, W. 2002. "Effect of Pore Structure, Randomness, and Size on Effective Mass Diffusivity." *AICE J* 48 (1): 15-24.

[12] Rahimi, P., and Ward, C. A. 2005. "Kinetics of Evaporation: Statistical Rate Theory Approach." *Int. J. Thermodyn.* 8: 1-14.

[13] Geankoplis, C. J. 2006. *Procesos de Transporte y Principios de Procesos de Separación*. 4th Spanish ed., México: Compañía Editorial Continental, 589-94.

[14] Weisz, P. B. 1995. "Molecular Diffusion in Microporous Materials: Formalisms and Mechanisms." *Ind. Eng. Chem. Res.* 34: 2692-9.

[15] De Gennes, P.-G., Brochard-Wyart, F., and Quéré, D. 2004. *Capillarity and Wetting Phenomena*. New York: Springer, 21.

[16] Bondi, A. 1964. "Van der Waals Volumes and Radii." *J.*

Phys. Chem. 68: 441-51.

[17] Hildebrand, J. H., and Scott, R. L. 1964. *The Solubility of Nonelectrolytes*. 3rd ed., New York: Dover.

[18] Sharma, S., and Debenedetti, P. G. 2012. "Evaporation Rate of Water in Hydrophobic Confinement." *Proc. Natl. Acad. Sci. (USA)* 109: 4365-70.

[19] Weijs, J. H., Marchand, A., Andreotti, B., Lohse, D., and Snoeijer, J. H. 2011. "Origin of Line Tension for a Lennard-Jones Nanodroplet." *Phys. Fluids* 23: 022001.

[20] Vasanthi, R., Bhattacharyya, S., and Bagchi, B. 2002. "Anisotropic Diffusion of Spheroids in Liquids: Slow Orientational Relaxation of the Oblates." *J. Chem. Phys.* 116: 1092-6.

[21] Chan, T, C., Li, H. T., and Li, K. Y. 2015. "Effects of Shapes of Solute Molecules on Diffusion: A Study of Dependences on Solute Size, Solvent, and Temperature." *J. Phys. Chem. B* 119: 15718-28.

[22] Ghorai, P. Kr., Yashonath, S., Demontis, P., and Suffritti, G. B. 2003. "Diffusion Anomaly as a Function of Molecular Length of Linear Molecules: Levitation Effect." *J. Am. Chem. Soc.* 125: 7116-23.

[23] Song, C., Garcés, J. M., and Sugi, Y. 2003. *Shape-Selective Catalysis*, *ACS Symposium Series*. Washington, DC: American Chemical Society.